Human Molecular Genetics, 2008, Vol. 17, No. 11 **1556–1568**
doi:10.1093/hmg/ddn043
Advance Access published on February 11, 2008

Mice deficient in Neu4 sialidase exhibit abnormal ganglioside catabolism and lysosomal storage

Volkan Seyrantepe[1], Maryssa Canuel[3], Stéphane Carpentier[4,5], Karine Landry[1], Stéphanie Durand[1], Feng Liang[1], Jibin Zeng[3], Aurore Caqueret[1], Roy A. Gravel[6], Sergio Marchesini[7], Claudia Zwingmann[2], Jacques Michaud[1], Carlos R. Morales[3], Thierry Levade[4,5] and Alexey V. Pshezhetsky[1,3,*]

[1]Department of Medical Genetics, CHU Sainte-Justine and [2]CHUM, University of Montreal, Montreal, Quebec, Canada, [3]Department of Anatomy and Cell Biology, Faculty of Medicine, McGill University, Montreal, Quebec, Canada, [4]INSERM U858, Laboratoire de Biochimie 'Maladies Metaboliques', CHU Toulouse, France, [5]Institut de Médecine Moléculaire de Rangueil, Université Toulouse III Paul-Sabatier, Equipe 14, IFR31, Toulouse, France, [6]Department of Biochemistry and Molecular Biology, University of Calgary, Calgary, Alberta, Canada and [7]Department of Biomedical Sciences and Biotechnologies, University of Brescia, Italy

Received October 16, 2007; Revised February 1, 2008; Accepted February 7, 2008

Mammalian sialidase Neu4, ubiquitously expressed in human tissues, is located in the lysosomal and mitochondrial lumen and has broad substrate specificity against sialylated glycoconjugates. To investigate whether Neu4 is involved in ganglioside catabolism, we transfected β-hexosaminidase-deficient neuroglia cells from a Tay-Sachs patient with a Neu4-expressing plasmid and demonstrated the correction of storage due to the clearance of accumulated GM2 ganglioside. To further clarify the biological role of Neu4, we have generated a stable loss-of-function phenotype in cultured HeLa cells and in mice with targeted disruption of the *Neu4* gene. The silenced HeLa cells showed reduced activity against gangliosides and had large heterogeneous lysosomes containing lamellar structures. *Neu4*$^{-/-}$ mice were viable, fertile and lacked gross morphological abnormalities, but showed a marked vacuolization and lysosomal storage in lung and spleen cells. Lysosomal storage bodies were also present in cultured macrophages preloaded with gangliosides. Thin-layer chromatography showed increased relative level of GD1a ganglioside and a markedly decreased level of GM1 ganglioside in brain of *Neu4*$^{-/-}$ mice suggesting that Neu4 may be important for desialylation of brain gangliosides and consistent with the *in situ* hybridization data. Increased levels of cholesterol, ceramide and polyunsaturated fatty acids were also detected in the lungs and spleen of *Neu4*$^{-/-}$ mice by high-resolution NMR spectroscopy. Together, our data suggest that Neu4 is a functional component of the ganglioside-metabolizing system, contributing to the postnatal development of the brain and other vital organs.

INTRODUCTION

Emerging evidence suggests that polysialylated and monosialylated glycolipids (gangliosides) play important roles in embryogenesis, development, immune response, signal transduction and cell death (reviewed in 1–4). Catabolism of gangliosides involves desialylation catalyzed by neuraminidases (or sialidases). Mammalian sialidases are encoded by the *Neu1, Neu2, Neu3* and *Neu4* genes, the products of which vary in subcellular location, tissue distribution, expression level and specificity. Neu1 is a component of the lysosomal multienzyme complex along with β-galactosidase (GAL) and the lysosomal carboxypeptidase, cathepsin A (CathA), which stabilizes the catalytically active conformation of Neu1 and protects it against rapid proteolytic degradation in the lysosome (reviewed in 5). Inherited deficiency of *Neu1*

*To whom correspondence should be addressed at: Service de génétique médicale, CHU Sainte-Justine, 3175 Côte Ste-Catherine, Montréal, Quebec, Canada H3T 1C5. Tel: +1 5143454931/2736; Fax: +1 5143454766; Email: alexei.pchejetski@umontreal.ca

causes the severe multisystemic neurodegenerative disorder, sialidosis. A clinically similar disorder, galactosialidosis, is caused by secondary Neu1 deficiency due to genetic defects in *CathA*. In both disorders, patients present with coarse facies, hepatosplenomegaly, dysostosis multiplex, bilateral macular cherry-red spots, mental and motor retardation (reviewed in 6,7) and show tissue storage and urinary excretion of sialyloligosaccharides and sialoglycopeptides.

Neu2 is a cytosolic protein found mostly in skeletal muscles and is active against α2-3-sialylated oligosaccharides, glycopeptides and gangliosides (8–10). The exact biological role of this enzyme is not known, but it was suggested to cleave G_{M3} ganglioside, associated with the cytoskeleton, leading to the alteration of cytoskeletal functions (11–13). Neu3 is a ubiquitously expressed integral membrane protein localized in caveolae microdomains of plasma membranes (14–16). Its highest expression is found in adrenal gland, skeletal muscles, heart, testis and thymus (14,15). The enzyme is active mostly against gangliosides, including G_{M1} and G_{D1a} (17). Neu3 is probably involved in the modulation of the oligosaccharide chains of gangliosides on the cell surface in the course of transformation, differentiation and formation of cell contacts (18,19). In particular, it is implicated in cell signaling during neuritogenesis (20), carcinogenesis and apoptosis (21), as well as in insulin signaling (22).

The physiological role of the recently identified sialidase Neu4, an enzyme ubiquitously expressed in human tissues is not clear. We showed that Neu4 is located in the lysosomal lumen and that it has a broad substrate specificity against glycoproteins, oligosaccharides and sialylated glycolipids. This raised the question of a potential overlap of biological functions between Neu4 and Neu1 (23). In contrast, others have shown that the majority of Neu4 is targeted to the inner and outer mitochondrial membranes and proposed that this enzyme may be involved in the cleavage of G_{D3} ganglioside in the mitochondria of apoptotic cells (24). Here we report that cultured HeLa cells stably transfected with Neu4 siRNA, as well as mice with targeted disruption of the *Neu4* gene, show partially impaired catabolism and lysosomal storage of gangliosides suggesting that Neu4 is a critical functional component of the ganglioside metabolizing system.

RESULTS

Neu4 catalyzes the conversion of gangliosides and compensates for β-hexosaminidase a deficiency

Previously, we and others have shown that in the presence of detergents, Triton X-100 or sodium cholate, Neu4 is highly active against a broad range of ganglioside substrates (23,24). Here we demonstrate that Neu4-transfected cells show sialidase activity against G_{D1a}, G_{M3} and G_{M2} gangliosides similar to that of the cells transfected with Neu3 sialidase and much higher than that of the cells transfected with Neu1 sialidase (Supplementary Material, Fig. S1). The activity of Neu4 but not of Neu3 towards G_{M3} and G_{D1a} gangliosides was significantly increased by the sphingolipid activator proteins saposins or G_{M2} activator protein (reviewed in 25), membrane-perturbing and lipid-binding proteins that facilitate glycolipid digestion in the lysosome (Supplementary Material, Fig. S1).

The activity of Neu4 against gangliosides was further studied using immortalized neuroglia cells from a Tay-Sachs patient that accumulates G_{M2} ganglioside in culture due to the genetic deficiency of lysosomal β-hexosaminidase A (26). Immortalized neuroglia cells derived from normal controls and from the Tay-Sachs patient as well as Tay-Sachs cells transfected with the Neu4-expressing plasmid (23) were cultured in the presence of [^{14}C]serine, [^{3}H]-labeled dihydroganglioside G_{M2} or fluorescently (lissamine–rhodamine) labeled G_{M1} ganglioside (27) to metabolically label the gangliosides. Chromatographic (TLC) analysis of the gangliosides performed after 48 h of loading with the dye-labeled G_{M1} (Fig. 1A) showed that normal control cells converted the dye-labeled G_{M1} to G_{M2} and further to lactosylceramide. Tay-Sachs cells also generated G_{M2} but failed to progress to lactosyl ceramide, presumably due to the block in β-hexosaminidase A activity. In contrast, the Neu4-transfected Tay-Sachs cells showed fully restored synthesis of lactosylceramide, presumably via glycolipid G_{A2}. Similar results were obtained on cells incubated with [^{3}H]-labeled dihydroganglioside G_{M2} instead of the fluorescent G_{M1}. Control cells contained the radiolabeled metabolites of G_{M2} ganglioside, including glycolipid G_{A2}, G_{M3} ganglioside, lactosylceramide, glucosylceramide and ceramide (represented as 'G_{A2}, G_{M3} and metabolites', Fig. 1B), while, as before, the Tay-Sachs cells were blocked at the level of G_{M2} ganglioside. Neu4-transfected Tay-Sachs cells showed a ganglioside pattern similar to that of the normal control cells, indicating that ganglioside catabolism was successfully restored (Fig. 1B). Similar observations were made when, instead of loading with labeled gangliosides, the cells were metabolically labeled with [^{14}C]serine. In this case, expression of Neu4 in the Tay-Sachs cells increased the level of glycolipid G_{A2} and G_{M2} catabolites almost 2-fold, while reducing the level of G_{M1} and G_{M2} gangliosides (Supplementary Material, Fig. S2). In turn, the microscopic examination of the Tay-Sachs neuroglia cells loaded with the total ganglioside mixture from porcine brain (∼44% G_{T1b}; ∼31% G_{D1a}; ∼16% G_{D1b}; ∼8% G_{M1} and trace amounts of other gangliosides, including G_{M2} and G_{M3}) showed the presence of multiple vacuoles, characteristic of lysosomal storage, whereas the lysosomes in Neu4-transfected neuroglia cells had homogeneous electron-dense content, indicating the correction of the organellar pathology as a result of reduction of accumulated G_{M2} ganglioside (Fig. 1C and D).

Neu4 silencing by RNA interference results in lysosomal storage and reduction of the total ganglioside sialidase activity

We next generated a stable loss-of-function phenotype in HeLa cells that express all four mammalian sialidases according to the RT–PCR data (data not shown). In order to suppress the expression of the *Neu4* gene, we used the pSilencer 4.1-CMV-Neo vector containing a 19-bp fragment from the human Neu4 cDNA [nucleotides 901–919 (23)] separated by a short 9-nucleotide spacer that forms the hairpin, followed by the reverse complement of the same sequence (pSilencer

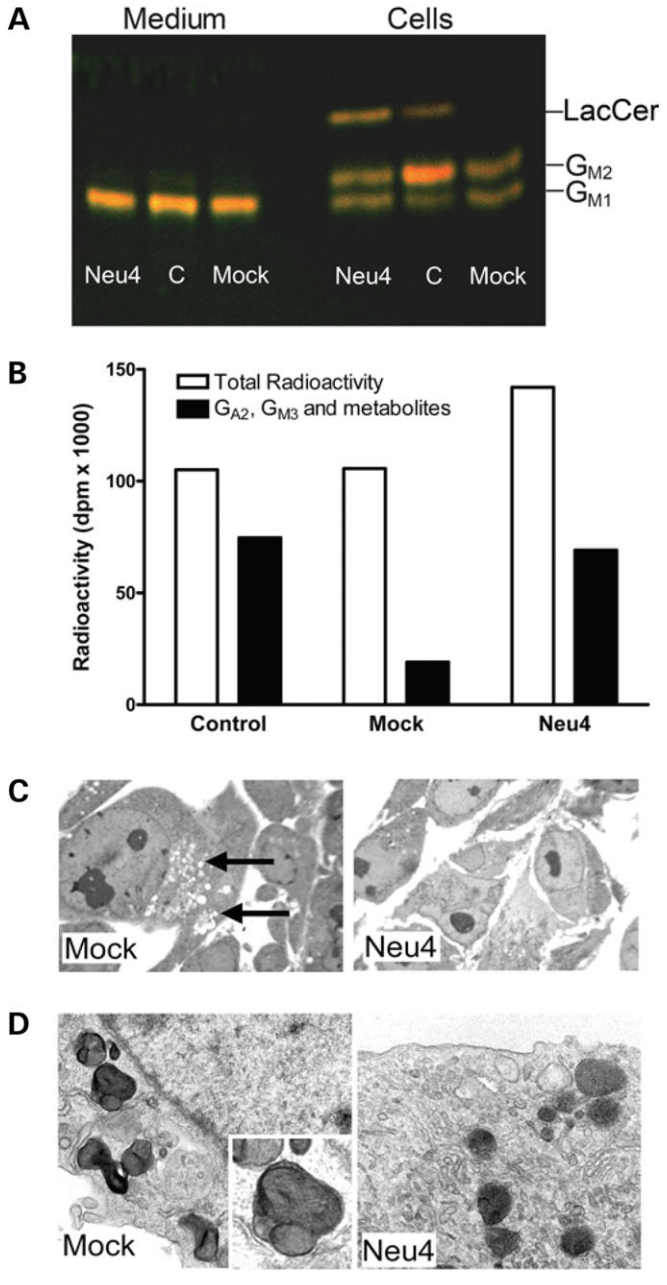

Figure 1. Effect of Neu4 transfection on cultured neuroglia cells from a Tay-Sachs patient. (**A**) TLC analysis of the gangliosides extracted from the culture medium (Medium) or from the cell homogenates (Cells) of the control neuroglia cells (C) or the cells from a Tay-Sachs patient transfected with pCMV-Neu4 (Neu4) and empty pCMV (Mock) plasmids. The cells were incubated in the presence of full medium containing 10% fetal calf serum and 3.3 nmol/ml of lissamine–rhodamine-labeled G_{M1} ganglioside for 72 h. The culture medium almost exclusively contains labeled G_{M1} ganglioside. Control cells, contain the labeled G_{M1} and G_{M2} gangliosides as well as lactosylceramide (LacCer), whereas in the Tay-Sachs cells the conversion stops at the level of G_{M2} ganglioside. Neu4-transfected Tay-Sachs cells show a ganglioside pattern similar to that of the normal control cells. (**B**) Ganglioside metabolism in neuroglia cells loaded with [^{3}H]-labeled dihydroganglioside G_{M2}. The cells were labeled in the presence of full medium containing 10% fetal calf serum and 10 μCi/ml of [^{3}H]-labeled G_{M2} 72 h. Histograms show the total amount of radioactivity found in glycolipids on the TLC plates and the amount of radioactivity associated with glycolipid G_{A2}, G_{M3} ganglioside and its metabolites (LacCer, GlcCer) in the extracts from the control neuroglia cells (Control) or the cells from a Tay-Sachs patient transfected with pCMV-Neu4 (Neu4) and empty pCMV (Mock) plasmids. Amounts of radioactivity associated with individual glycolipids are shown in Supplementary Material, Table S1. (**C**) Light micrographs of neuroglia cells from a Tay-Sachs patient loaded for 72 h with total porcine brain gangliosides (0.2 mg/ml of medium). Mock-transfected cells are filled with vacuoles (arrows). Neu4-transfected cells are devoid of vacuoles. Magnification ×1200. (**D**) Electron micrographs of neuroglia cells from a Tay-Sachs patient loaded with total porcine brain gangliosides. Mock-transfected cells contained mainly abnormal lysosomes showing vesicular profiles which differ in shape and size and are sometimes lamellated (inset). In the Neu4-transfected cells the majority of the lysosomes present homogeneous electrondense content typical of normal structures. Magnification ×35 000.

4.1-Neu4). Similarly, the pSilencer 4.1-Neu1 vector contained nucleotides 525–543 from the human Neu1 cDNA. HeLa cells were transfected with the pSilencer 4.1-Neu4 or pSilencer 4.1-Neu1 vectors, as well as mock vectors containing scrambled DNA. Colonies arising from Geneticin (G-418)-resistant cells were selected, expanded into cell lines and tested for the expression of the *Neu1* and *Neu4* mRNA by RT–PCR, which showed at least 80% reduction in the cells treated with pSilencer 4.1-Neu1 or pSilencer 4.1-Neu4 vectors when compared with the mock-treated controls (data not shown). The sialidase activity assayed in the lysates using 4MU-NeuAc was reduced by 15–35%, probably reflecting the input of the redundant activity of the remaining three sialidases. However, the cells transfected with the Neu4 siRNA showed a statistically significant reduction of sialidase activity measured with total porcine gangliosides as substrate (Fig. 2A). When the cells were further loaded for 48 h with total gangliosides and examined by light microscopy, we have observed extensive vacuolization in the cells treated with pSilencer 4.1-Neu4 vector, but not in the mock-treated cells (Fig. 2B). Electron microscopy revealed that these cells had large heterogeneous lysosomes containing lamellar structures indicating lysosomal storage due to the suppressed Neu4 expression (Fig. 2C). The lysosomal storage was also observed in immortalized normal human neuroglia cells treated with the *Neu4* siRNA (Supplementary Material, Fig. S3) showing that this phenomenon is not restricted to a particular cell type.

Abnormal catabolism of gangliosides in Neu4 knockout mice

Generation of Neu4-deficient mice. To define the physiological role of Neu4, we generated a mouse model with targeted disruption of the *Neu4* gene. To produce the *Neu4* null mice, a PGK-neomycin expression cassette was inserted into exon 3 of the mouse *Neu4* gene (Fig. 3A and B). Northern blot analysis with a total mouse Neu4 cDNA as a probe revealed the 1.4-kb *Neu4* transcript in the brain tissues of the wild-type mouse (Fig. 3C). In contrast, no mature or aberrant *Neu4* mRNA was detected in the $Neu4^{-/-}$ mice (Fig. 3C). The absence of the *Neu4* transcript in the total RNA extracted from the brain of $Neu4^{-/-}$ mice was also confirmed by RT–PCR, whereas wild-type and $Neu4^{-/-}$ mice showed no difference in the level of Neu1 transcript (Fig. 3D) as well as in the level of Neu2 and Neu3 transcripts (data not shown). Heterozygous mating yielded $Neu4^{-/-}$ progeny in the frequency expected from Mendelian inheritance,

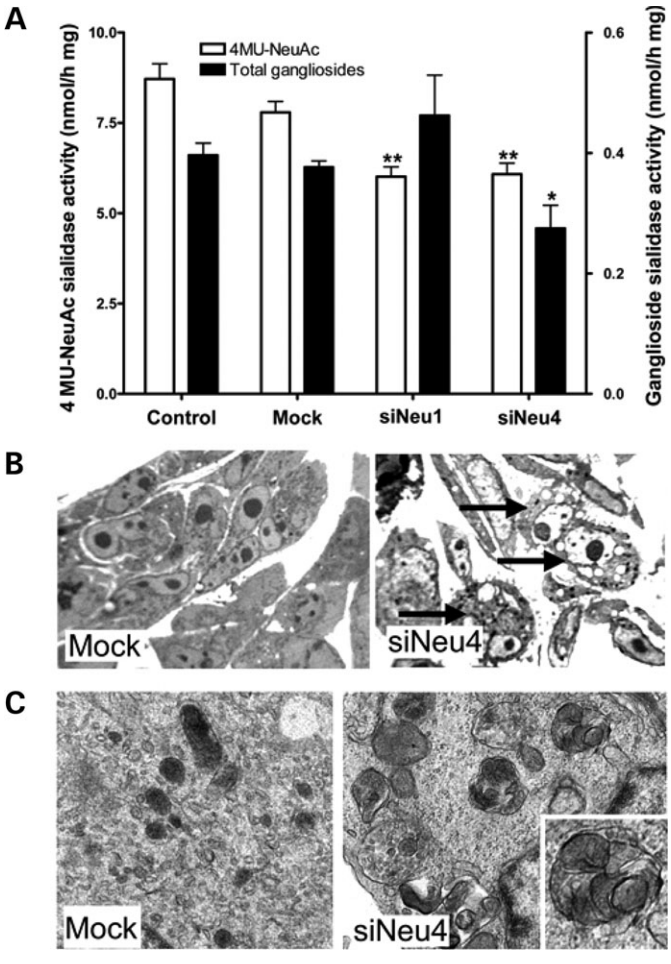

Figure 2. Effect of Neu4 and Neu1 silencing in HeLa cells. (**A**) Sialidase activity in lysates of non-transfected HeLa cells (Control) and the cells stably transfected with pSilencer-Neu1 (siNeu1), pSilencer-Neu4 (siNeu4) or pSilencer (Mock) vectors against the total porcine brain gangliosides or against the artificial sialidase substrate, 4MU-NeuAc. Values represent means ± SD of triplicate experiments. $^{*}P < 0.05$ and $^{**}P < 0.01$ when compared with the mock-transfected cells. Effect of the Neu4 silencing on the cell morphology as seen on light (**B**) and electron (**C**) micrographs. HeLa cells transfected with pSilencer-Neu4 and loaded for 72 h with 0.2 mg of total gangliosides from porcine brain per milliliter of medium present the extensive vacuolation (**B**, arrows) and are filled with large vacuoles containing vesicular profiles (**C**, inset). Mock-transfected HeLa cells loaded with gangliosides do not present vacuolation (B) and contain normal lysosomes (C). Magnification 1200 (B) and ×35 000 (C). All microphotographs represent typical images obtained in triplicate experiments; from 70 to 150 cells were studied for each condition in each experiment.

suggesting that the disrupted *Neu4* allele does not cause embryonic lethality. The *Neu4*$^{-/-}$ mice grow normally and have a normal lifespan. Both males and females are fertile and can be bred to each other to produce knockout litters.

Effect of the Neu4 deficiency on sialidase activity in mouse tissues. Sialidase activity towards 4MU-NeuAc and porcine brain gangliosides was tested in total homogenates and subcellular organelle fractions from liver, kidney, spleen, lungs, heart muscle and brain of wild-type and *Neu4*$^{-/-}$ mice. Consistently with the previous data which showed that in mouse Neu4 is expressed almost exclusively the in brain (28), we observed statistically significant ∼30% reduction of sialidase activity measured with total gangliosides or with 4MU-NeuAc in the organellar fractions from brain of *Neu4*$^{-/-}$ mice (Table 1) containing the majority of lysosomes according to β−hexosaminidase and β−glucosidase assays (data not shown). The reduction most probably reflects the proportion of the activity that is lost due to the Neu4 defect, the rest representing the activities of Neu3 and Neu1 sialidases, which are also active at acidic pH and abundant in brain tissue. The ganglioside sialidase activity of the microsomal fraction containing the majority of Neu3 remained unchanged in the *Neu4*$^{-/-}$ mice (data not shown). There was no significant difference in sialidase activity measured with either gangliosides or 4MU-NeuAc between the wild-type and *Neu4*$^{-/-}$ mice in other tissues (data not shown), which is consistent with the low level of the Neu4 transcript observed in these organs by northern blotting (28).

Pathology of Neu4$^{-/-}$ *mice reveals lysosomal storage*. Pathological examination of *Neu4*$^{-/-}$ mice carried out at the age of 4 weeks did not reveal any gross changes in the visceral organs, however, microscopic investigation of tissue sections (Fig. 4A) revealed a marked vacuolization of the lungs and spleen consistent with lysosomal storage phenotype. While cells from wild-type mice showed dense lysosomes, the cells from *Neu4*$^{-/-}$ mice contained light vacuoles different from normal lipid granules stained with toluidine blue, confirming our hypothesis that Neu4 participates in lysosomal lipid catabolism. Further, electron microscopic analysis revealed that in the spleen storage occurs in the red pulp and that the affected cells include macrophages and lymphocytes (Fig. 4B). Splenocytes isolated from the knockout mice differentiated in culture into macrophages. When loaded with the total porcine gangliosides, they also exhibited a marked accumulation of heterogeneous lysosomes. Between 10 and 50% of the lysosomes contained lamellated membrane-like structures and/or membrane-like whorls. Splenocytes isolated from the wild-type littermates also loaded with gangliosides contained a homogeneous population of electron dense lysosomes, which were devoid of membrane-like structures (Fig. 4C).

In lungs of *Neu4*$^{-/-}$ mice at 4 weeks of age, storage was observed mostly in septal macrophages (Fig. 4D). Nevertheless, at 6 months, the lungs of the mutant mice presented a normal histological appearance when compared with the wild-type lungs. The bronchioles were lined by ciliated and clara cells and the lung alveoli by type I and II pneumocytes which did not exhibit morphological abnormalities. However, the lamellar bodies in type II pneumocytes of lungs in the *Neu4*$^{-/-}$ mice were larger in diameter (mean diameter 0.8 μm ± 0.1 μm) than those in the lungs of the wild-type mice (mean diameter 0.4 μm ± 0.05 μm) (Fig. 4E). No apparent pathological changes were observed in the brain, heart and liver of the *Neu4*$^{-/-}$ mice at the age of 1, 4 or 8 months.

The Neu4$^{-/-}$ *mice show altered patterns of tissue gangliosides and other lipid-related metabolites*. To test whether the inclusion bodies present in the *Neu4*$^{-/-}$ mice contain gangliosides, ganglioside composition of the brain, liver, kidney, spleen and lung tissues from the 1-month-old and 9-month-old

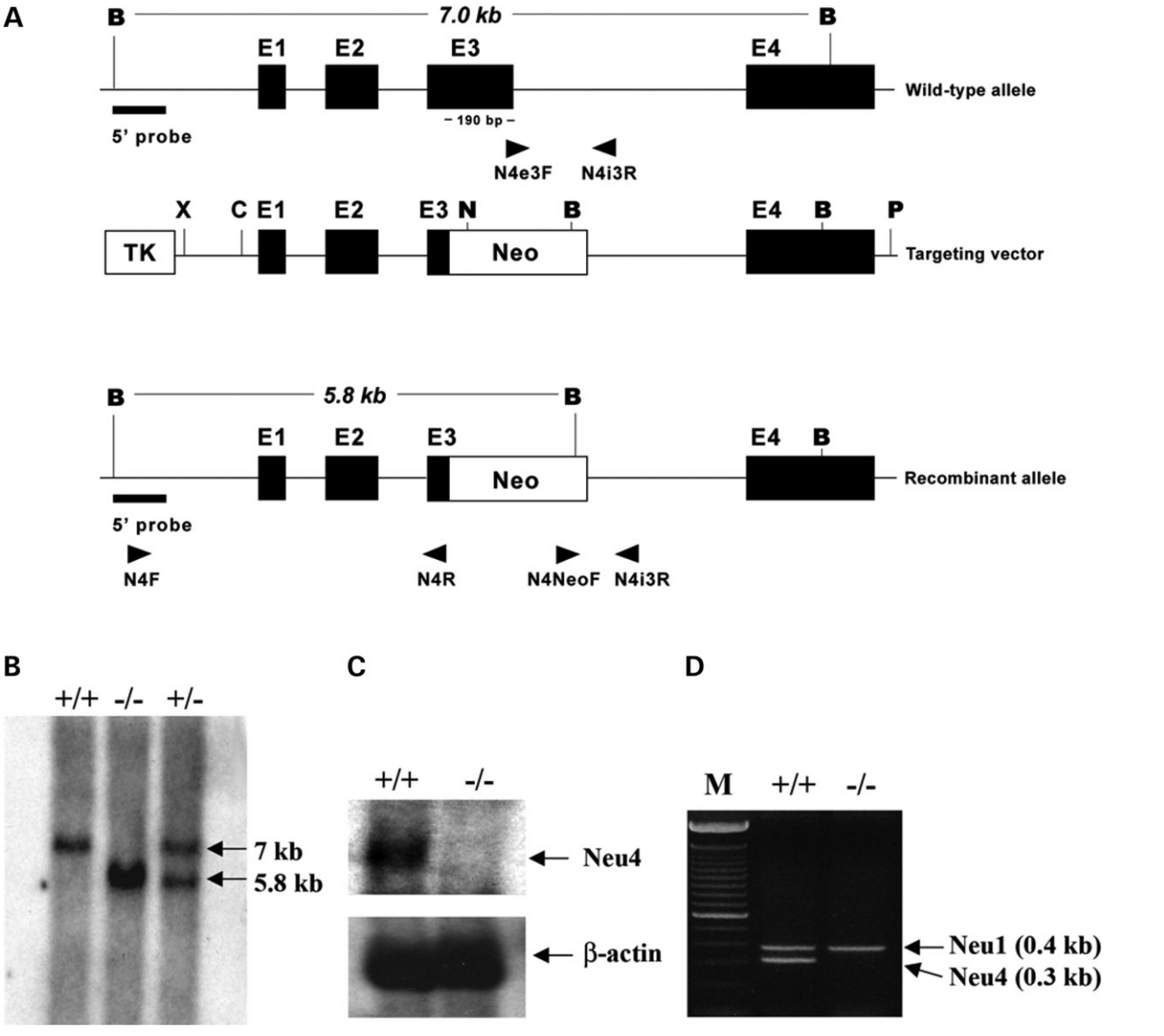

Figure 3. Generation of the *Neu4*$^{-/-}$ mice. (**A**) Strategy for producing the targeted disruption of the Neu4 gene. In the targeting vector, the 190 bp fragment of the exon 3 containing nucleotides 112–175 was replaced with a Neo cassette. Exons in the mouse *Neu4* gene are shown as black, numbered boxes and *PGK-neomycin* (*Neo*) and *HSV thymidine kinase* (*TK*) genes as white boxes. Restriction sites are indicated as **B** (*BamH*I), **P** (*Pac*I), **X** (*Xho*I), **C** (*Cla*I) and **N** (*Not*I). Primers (N4F, N4R, N4NeoF, N4e3F and N4i3R) were used for genotyping the ES clones and mice by PCR. (**B**) The genotype of F2 progeny at the Neu4 locus was determined by Southern blot hybridization using the 5'-flanking probe. After the digestion of tail genomic DNA by *BamH*I, a 5.8-kb band was diagnostic of a targeted Neu4 allele (−/−) and the wild-type allele (+/+) was identified by a 7.0-kb band. (+/−), heterozygous animal. (**C**) Northern blot analysis of the total brain from the wild-type (+/+) and *Neu4*$^{-/-}$ (−/−) mice hybridized with the cDNA probe for the mouse *Neu4*. Neu4 mRNA was not detected in the brain RNA from the *Neu4*$^{-/-}$ mice. (**D**) RT–PCR detects normal levels of the Neu4 and Neu1 mRNA in the brain of wild-type (+/+) mice, whereas only Neu1 message is detected in the brain of *Neu4*$^{-/-}$ (−/−) animals.

Neu4$^{-/-}$ and wild-type littermates was analyzed by thin-layer chromatography (TLC). At both ages, increased relative levels of polysialylated gangliosides (such as G_{D1a}) were found in spleen, lungs and brain and reduced relative levels of G_{M1} ganglioside in lungs and brain of *Neu4*$^{-/-}$ mice (Fig. 5A). The most pronounced difference between the *Neu4*$^{-/-}$ and the wild-type mice was in the ratio of G_{M1} to G_{D1a} in brain (Fig. 5B). At the same time no differences in lipid patterns were observed in liver or kidney tissues (data not shown).

To detect the potential changes in the levels of other metabolites, we performed analyses of organic and aqueous extracts of the lung, liver and the spleen tissues of *Neu4*$^{-/-}$ and wild-type mice by high-resolution NMR spectroscopy. The fully relaxed ^{1}H NMR spectra showed changes in the concentration of several lipid-related metabolites in lungs and spleen. In particular, a ∼10-fold increase of cholesterol, phosphatidylcholine, ceramide and at least 2-fold increase of polyunsaturated fatty acids was demonstrated in the lungs of *Neu4*$^{-/-}$ mice (Supplementary Material, Fig. S4). A

Table 1. Sialidase activity in the subcellular fractions from brain of the wild-type and *Neu4*-deficient mice

Fraction	Specific sialidase activity (nmol/h mg) 4MU-NeuAc		Total gangliosides	
	$Neu4^{+/+}$	$Neu4^{-/-}$	$Neu4^{+/+}$	$Neu4^{-/-}$
Post-nuclear supernatant	1.2 ± 0.07	1.05 ± 0.05	1.3 ± 0.4	1.2 ± 0.4
Heavy organellar fraction	1.32 ± 0.07	0.84 ± 0.03[a]	0.78 ± 0.05	0.59 ± 0.01[a]
Light organellar fraction	2.4 ± 0.24	1.6 ± 0.08[a]	0.61 ± 0.02	0.41 ± 0.01[a]

The data show mean values ± SE of triplicate experiments performed with 2 mice in each group.
[a]Significantly different from $Neu4^{+/+}$ ($P < 0.05$ using two-tailed *t*-test).

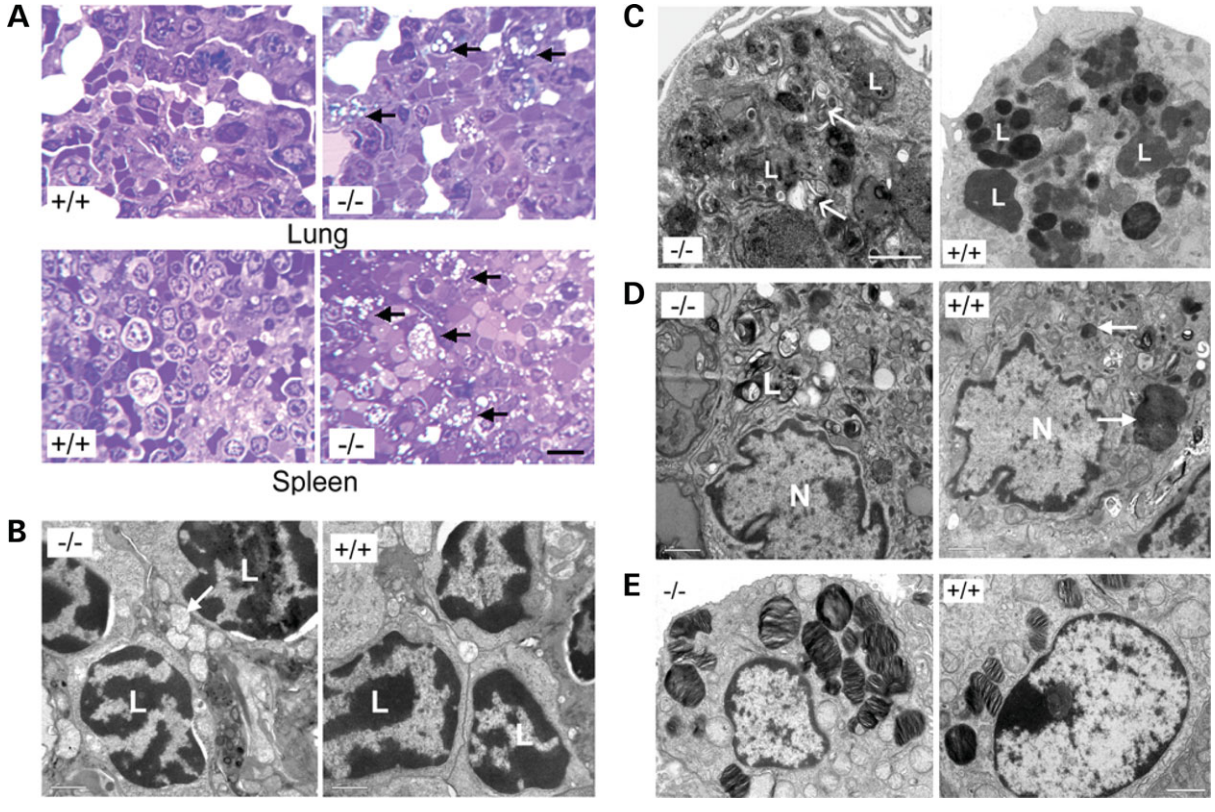

Figure 4. Pathological changes in Neu4-deficient mice. (**A**) Microscopic investigation of tissue sections from lungs and spleen shows a marked vacuolization in the $Neu4^{-/-}$ mice consistent with the lysosomal storage phenotype. While the cells from the wild-type mouse show dense lysosomes stained with osmium the cells from the $Neu4^{-/-}$ mice contain light vacuoles (arrows) different from the normal lipid granules stained with toluidin blue. Magnification ×1200; bar equals 12 μm and applies to all images. (**B**) Electron micrographs showing a large accumulation of vacuoles in the cytoplasm of lymphocytes (L) in the red pulp of spleen from the $Neu4^{-/-}$ mouse (arrows). The cells from wild-type show homogeneous lysosomal content. Magnification ×8000; bar equals 1 μm. (**C**) Electron micrographs of cultured splenocyte-derived macrophages supplemented with gangliosides. The cells from the knockout mice show a heterogeneous population of lysosomes (L) and a moderate accumulation of lysosomes containing lamellated or whorls of membrane-like structures (arrows). The wild-type splenocytes show a homogenous population of lysosomes (L). N, nucleus. Magnification ×16 000; bar equals 1 μm. (**D**) Electron micrographs of septal macrophages from lungs of wild-type and knockout mice. Wild-type macrophages show a homogenous population of lysosomes (arrows). Conversely, knockout macrophages present a moderate accumulation of lysosomes containing whorls of membrane (L). N, nuclei of septal macrophages. Magnification ×10 000; bar equals 1 μm. (**E**) Electron micrograms of Type II pneumocytes from the lungs of the wild-type and knockout mice. The lamellar bodies in the cells of $Neu4^{-/-}$ mice are larger in diameter (mean diameter 0.8 μm ± 0.1 μm) than those in the lungs of the wild-type mice (mean diameter 0.4 μm ± 0.05 μm). Magnification ×20 000; bar equals 1 μm.

~10-fold increase of an unknown peak, likely corresponding to a modified ceramide, was also observed. The cholesterol, ceramide and fatty acid levels were similarly increased in the spleen of $Neu4^{-/-}$ mice but remained unaltered in the liver (data not shown). Blood levels of cholesterol and fatty acids were normal (not shown). No difference in the composition of urinary oligosaccharides between normal and $Neu4^{-/-}$ mice could be detected by TLC (not shown).

Brain expression of Neu4 and behavioral analysis of Neu4-deficient animals. Previous northern blot analysis showed that in mouse *Neu4* is expressed in the brain at a higher

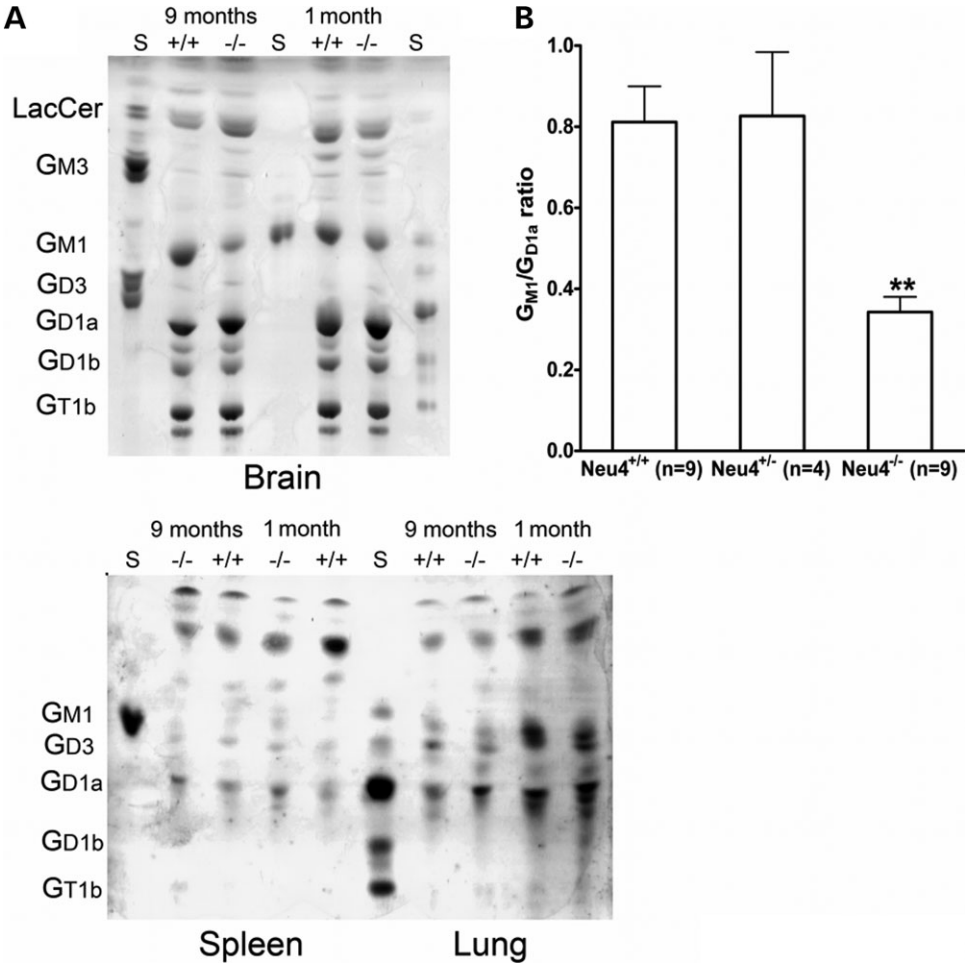

Figure 5. Alteration of ganglioside metabolism in the tissues of Neu4-deficient mice. (**A**) Representative TLC images of orcinol-stained gangliosides from brain and resorcinol-stained gangliosides from lungs and spleen of the *Neu4*$^{+/+}$, and *Neu4*$^{-/-}$ animals at 1 and 9 months of age. The positions of the ganglioside standards (S) are indicated on the left. (**B**) Histograms show the ratio of G_{M1} and G_{D1a} gangliosides as measured by TLC in the extracts of brain tissues from *Neu4*$^{+/+}$; *Neu4*$^{+/-}$ and *Neu4*$^{-/-}$ mice. Values represent means $\pm$ SD of duplicate measurements.$^{**}P<0.01$ when compared with the *Neu4*$^{+/+}$ or *Neu4*$^{+/-}$ animals by the two-tailed *t*-test.

level than in other tissues (28). To address the distribution of *Neu4* mRNA in the brain, we analysed coronal sections of newborn brain by *in situ* hybridization and found that *Neu4* expression was undetectable (data not shown). In contrast, *Neu4* was strongly expressed in scattered cells found in all regions of the brain in 7-week-old mice (Supplementary Material, Fig. S5C,D,G,H) with a distribution similar to that of microglia cells (data not shown). In addition, weak *Neu4* expression was detectable ubiquitously. In the same mice *Neu1* was expressed ubiquitously throughout the brain but more strongly in some areas such as the CA3 region of the hippocampus (Supplementary Material, Fig. S5A) and the cortex (Supplementary Material, Fig. S5E). *Neu3* expression was almost undetectable and did not show a specific pattern (Supplementary Material, Fig. S5B and F).

To determine if the altered ganglioside pattern in the brain of the *Neu4*$^{-/-}$ mice was sufficient to result in behavioral deficits reflective of the loss of neurons and progressive neurodegeneration similar to that detected in other sphingolipidoses, we performed a behavioral examination of 2-month-old and 10-month-old siblings of both genotypes. Open field, water maze and rotarod tests were conducted. These are tests that have previously been effective in monitoring the progression of the disease in the mouse model of Tay-Sachs disease (29). While the outcomes were variable, *Neu4*$^{-/-}$ mice at both 2 and 10 months showed no deficits in any of these tests (Supplementary Material, Fig. S6). However, more in depth studies will be required to rule out subtle defects.

DISCUSSION

While Neu4 has been characterized in mouse and human tissues, the reports on subcellular localization and potential specific function of this enzyme have varied. The pH optimum of human and mouse Neu4 is extremely acidic, reported in the range of 3.2 to 4.8, as expected of a lysosomal hydrolase, although it has a minor neutral peak as well (23,24,30) which might account for the mitochondrial activity of Neu4 proposed by Yamaguchi *et al*. (24). In this study,

functional confirmation of the lysosomal localization of Neu4 came from the ability of the enzyme to fully correct the catabolism of G_{M2} ganglioside in Tay-Sachs neuroglia cells which accumulate G_{M2} ganglioside in their lysosomes (26,31). Resumption of G_{M2} catabolism following transfection with Neu4 required its expression in the lysosome in order to give it access to the substrate. This was demonstrated with fluorescently labeled G_{M1} ganglioside which was cleaved to G_{M2} in untreated cells and catabolized further to the lactosylceramide derivative in treated cells. Similarly, [^{3}H]-G_{M2} and [^{14}C]-serine tracer experiments confirmed the restored catabolism of G_{M2}, as did the loss of lysosomal swelling in the treated cells.

Historically, Neu1, as part of the β-galactosidase/Neu1/CathA complex has been regarded as the best candidate for a ganglioside sialidase. For example, it was previously reported that Neu1 is able to catalyze the hydrolysis of gangliosides in the presence of bile salts *in vitro* (17,32–34). However, the analysis of storage products in sialidosis and galactosialidosis patients, with functional deficiency of Neu1 (reviewed in 6,7) or in the corresponding knockout mouse models (35,36) did not reveal the accumulation of gangliosides. These findings suggest either that Neu1 is not essential for their catabolism or that redundant activities contribute to the desialylation of gangliosides *in vivo*. Our studies point to Neu4 as the source of the ganglioside activity. Indeed, unlike Neu1, Neu4 effectively hydrolyzed *in vitro* gangliosides in the presence of lysosomal sphingolipid activator proteins and transfection of HeLa cells with Neu4 siRNA, but not with Neu1 siRNA, reduced their ganglioside sialidase activity. Both Neu4 siRNA-transfected HeLa cells and neuroglia cells, but not untransfected cells, produced lysosomal storage bodies in response to loading with the mixed gangliosides. These data implicate Neu4 as a predominant ganglioside sialidase of lysosomal origin.

Our results in cell cultures extend to a knockout mouse model of Neu4 deficiency. Ganglioside patterns for the liver, lungs and brain of *Neu4*$^{-/-}$ mice differed significantly from those of their wild-type littermates. In the knockout model, we observed a markedly decreased ratio of G_{M1} to G_{D1a} gangliosides suggesting that Neu4 is primarily involved in the desialylation of the latter lipid. We have also detected increased concentrations of other lipids such as cholesterol, ceramide and phospholipids in liver and lungs, most probably caused by the alterations in their catabolism and trafficking secondary to the accumulation of sphingolipids, as observed in Niemann-Pick disease (37–39).

In the lungs and spleen of young (4 weeks to 4 months) animals, the elevated level of gangliosides and other lipids was accompanied by lysosomal storage, mostly affecting tissue macrophages. Lysosomal storage was also observed *ex vivo* when the splenocyte-derived macrophages from the *Neu4*$^{-/-}$ mice were loaded with total gangliosides. On the other hand, in contrast to many lysosomal enzymopathies, the lysosomal storage and vacuolization in the tissues of the *Neu4*$^{-/-}$ mice did not progress with age. Moreover, the microscopic examination of lungs and spleen from older (6–10 months of age) *Neu4*$^{-/-}$ mice showed generally a normal morphology, suggesting that the expression of the *Neu4* gene is particularly important during postnatal development.

In the lungs, the lamellar bodies in the type II pneumocytes of the *Neu4*$^{-/-}$ animals remained 2-fold enlarged even at 8 months of age. These organelles, which typically present concentric or parallel lamellae, are secretory granules containing phospholipids, glycosaminoglycans and surfactant proteins, synthesized by the type II pneumocytes. They are continuously formed and released at the luminal surface, providing an extrapulmonary coating of pulmonary surfactant that lowers the alveolar surface tension (reviewed in 40). The larger lamellar bodies observed in the Neu4 knockout animals is an intriguing feature that may indicate a potential induction of surfactant synthesis in the type II pneumocytes due to the absence of Neu4. Although this suggestion requires experimental verification, it is interesting to note that lamellar bodies often merge with multivesicular bodies and thus these structures are functionally related to lysosomes (reviewed in 41).

By *in situ* hybridization, Neu4 mRNA was shown to be strongly expressed in cells that are scattered in the mouse brain. The distribution of these cells is reminiscent of that of microglial cells, which infiltrate the developing CNS after P5 and participate in axon growth, vasculogenesis and apoptosis (reviewed in 42). The time course of the migration of microglial cells into the brain is consistent with that of *Neu4* expression, which sharply increases several days after birth and reaches a peak at several weeks of age (43). However, while the predominant expression is in microglia, *Neu4* appears to be expressed at low levels ubiquitously in the brain, so we cannot exclude the possibility that it is also produced at lower levels in other cell types, such as neurons, given its impact in diseases such as sialidosis and galactosialidosis where as we previously showed exogenous Neu4 eliminated undigested substrates and restored a normal morphological phenotype of the lysosomal compartment *in situ* (23).

An additional lysosomal disease which may be ameliorated by the lysosomal presence of Neu4 activity is the knockout mouse model of Tay-Sachs disease (44,45). The human disorder, with a carrier frequency of ∼1/30 in Ashkenazi Jews, is caused by mutation of the *HEXA* gene coding for the α-subunit of lysosomal β-hexosaminidase A. This enzyme converts G_{M2} to G_{M3} ganglioside. *Hexa*$^{-/-}$ mice, depleted of β-hexosaminidase A, remain asymptomatic to at least 1 year of age (29), owing to the ability of these mice to catabolize stored G_{M2} ganglioside via a lysosomal sialidase into glycolipid G_{A2}. G_{A2} is further processed by β-hexosaminidase B, to yield lactosylceramide (45), thereby completely bypassing the β-hexosaminidase A defect (Fig. 6). This bypass is not effective in humans, with the outcome that infantile Tay-Sachs disease is fatal in the first years of life. The tissue levels of Neu4 mRNA may provide an explanation for the difference in Tay-Sachs disease severity in humans and mice. Comelli *et al*. (28) showed Neu4 to be expressed at high level in mouse brain with only trace expression in other tissues. In contrast, expression in human tissues was more widely distributed, with brain levels lower than in other tissues (23,24,30). Strikingly, we show that transfection of human Tay-Sachs neuroglia cells with Neu4 produces a similar catabolism through G_{A2}, effectively 'treating' the disease through the same metabolic bypass that is so effective in the mouse

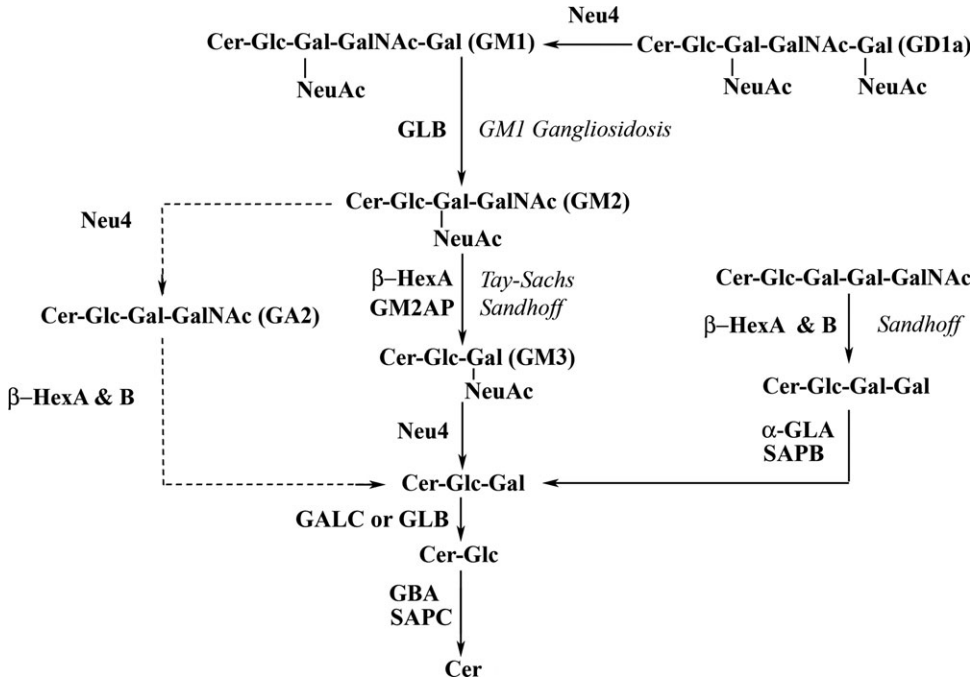

Figure 6. Ganglioside degradation pathways and genetic disorders associated with their defects in humans showing the proposed role of Neu4. The dotted line indicates the proposed alternative pathway for the hydrolysis of G_{M2} by Neu4 in the mouse to yield G_{A2} followed by its hydrolysis by ß-hexosaminidases A and/or B to yield lactosyl ceramide. Cer, ceramide; Gal, galactose; Glc, glucose; NeuAc, *N*-acetylneuraminic acid; GalNAc, *N*-acetylgalactosamine; Cer-Glc, glucocerebroside; Cer-Glc-Gal, lactosyl ceramide; GM1, D-galactosyl-*N*-acetyl-D-galactosaminyl-(*N*-acetylneuraminyl)-D-galactosyl-D-glucosylceramide; GM2, *N*-acetyl-D-galactosaminyl-(*N*-acetylneuraminyl)-D-galactosyl-D-glucosylceramide; GM3, (*N*-acetylneuraminyl)-D-galactosyl-D-glucosylceramide; GA2, *N*-acetyl-D-galactosaminyl-D-galactosyl-D-glucosylceramide; GBA, acid β-glucosidase; GLB, β-galactosidase; α-GLA, α-galactosidase A, GM2AP, GM2 activator protein; SAPB, saposin B; SAPC, saposin C.

model. It is attractive to speculate that stimulation of human Neu4, perhaps through drug-mediated induction or activation, could activate the bypass in human Tay-Sachs disease or could substitute for Neu1 in human sialidosis and galactosialidosis and provide treatments of these devastating diseases.

MATERIALS AND METHODS

Animals

Two fragments of the mouse Neu4 gene containing exons 1–3 (2630 bp) and intron 3-exon 4 (3060 bp) were amplified by PCR using the mouse genomic DNA (129svj) and the primer sets: 5-**CTC GAG** GGA AAC CCA GAG CAA TCT CA-3; 5-**ATC GAT** GGG CAA GGG TTC ATA GAC CT-3; and 5-**GCG GCC GC**C ATC TGA TGT GTG GGA TGG-3; 5-**TTA ATT AA**G GTC AGC CTG ATC TAC AGA GTG-3, respectively. The first fragment was subcloned between the *Neo* gene and the thymidine kinase (*TK*) gene into a pBluescript vector using the *Xho*I and *Cla*I restriction sites of the primers (bold). The second fragment was subsequently inserted into the 3′ region of the *Neo* cassette using the *Not*I and *Pac*I restriction sites. The final linearized targeting construct, shown in Figure 3A, was electroporated into R1 ES cells. G418-resistant (positive selection for the *Neo* gene) and Ganciclovir-resistant (negative selection for the *TK* gene) ES cells were screened for homologous recombination by PCR using the allele-specific primers pair: 5′-TGG TTT CTA ACT GGC CAA GG-3′ (N4F) and 5′-CCA CAC GCG TCA CCT TAA TA-3′ (N4R) as shown in Figure 3A. ES clones were further screened by Southern blot hybridization with genomic 5′-probe that were outside of the targeting construct (Fig. 3A). Targeted ES clones were then injected into C57BL/6H blastocysts and implanted into pseudo-pregnant females. The resulting male chimeras were crossed with C57BL/6J and offspring that received the ES genome was identified by the inheritance of the agouti coat color and genotyped by Southern blot hybridization using the 5′flanking probe as described in Figure 3B. Multiplex PCR primers 5′-CTC TTC TTC ATT GCC GTG CT-3′ (N4e3F) 5-GCC GAA TAT CAT GGT GGA AA-3′ (N4NeoF) and 5′-GAC AAG GAG AGC CTC TGG TG-3′ (N4i3R) were used to genotype mice in the F2 generation.

To document the absence of Neu4 gene expression, northern analysis was performed using 25 μg of total RNA extracted from the total frozen brain tissues of *Neu4*$^{-/-}$ and wild-type mice using the Trizol Reagent (Invitrogen). Denatured RNA mixed with ethidium bromide and separated by electrophoresis on a 1% (w/v) agarose gel containing 6% (v/v) formaldehyde was transferred onto Hybond N^+ filters (Amersham Biosciences) and fixed by UV cross-linking. The blots were hybridized in Rapid-hyb buffer (Amersham Biosciences) with a full length mouse Neu4 cDNA amplified from total mouse brain RNA by reverse transcription and radio-labeled with [α-^{32}P] dCTP using a Ready Prime Random Labeling Kit (Amersham Biosciences). The same probe was used with the commercial blots (Seegene Inc.) to examine *Neu4* RNA expression in

various mouse tissues. Expression of the *Neu4* and *Neu1* genes in mouse tissues was also analyzed by RT–PCR as described subsequently. The Neu4-deficient mice were compared with the appropriate littermate controls. All mice were bred and maintained in the Canadian Council on Animal Care (CCAC)-accredited animal facilities of the Ste-Justine Hospital Research Center according to the CCAC guidelines. Approval for the animal care and the use in the experiments was granted by the Animal Care and Use Committee of the Ste-Justine Hospital Research Center.

Transient expression of human sialidases in COS-7 cells

COS-7 cells cultured until 70% of confluency in MEM supplemented with 10% (v/v) fetal calf serum (Invitrogen) and antibiotics were transfected using a Lipofectamine Plus kit (Invitrogene) with the previously described plasmids containing cDNA of human sialidases pCMV-Neu1, pCMV-Neu3 and pCMV-Neu4, human cathepsinA/protective protein pCMV-CathA (23) and plasmids containing human prosaposin and G_{M2} activator proteins (46). Forty-eight hours after transfection cells were harvested and assayed for sialidase activity as described in what follows.

Stable transfection of HeLa and human neuroglia cells with the Neu4 and Neu1 gene silencing vector

The selection of the siRNA coding sequences was determined using insert design software tool from Ambion. Single stranded sense and antisense DNA oligonucleotides corresponding to the sequences of human Neu4 (5′-GAT CCC AGG CCA CGG GAT GAC AGT TTC AAG AGA ACT GTC ATC CCG TGG CCT GTTA-3′ and 5′-AGC TTA ACA GGC CAC GGG ATG ACA GTT CTC TTG AAA CTG TCA TCC CGT GGC CTGG-3′) and Neu1 (5′- GAT CCG GAT GAT GGT GTT TCC TGG TTC AAG AGA CCA GGA AAC ACC ATC ATC CTT-3′and 5′-AGC TTA AGG ATG ATG GTG TTT CCT GGT CTC TTG AAC CAG GAA ACA CCA TCA TCC-3′) cDNA were annealed and cloned into *Hind*III and *Bam*HI sites of the pSilencer 4.1-CMV-Neo expression vector (Ambion). The orientation of the inserts was verified by sequencing using vector-specific primers. HeLa and neuroglia cells cultured in antibiotic-free MEM supplemented with 10% FBS, 100 mM non-essential amino acids and 100 mM sodium pyruvate or human neuroglia cells cultured in Dulbecco's Modified Eagle's Medium (DMEM) with 10% FBS were transfected with pSilencer 4.1-Neu4 or pSilencer 4.1-Neu1 vectors, vectors containing scrambled DNA as well as with the pSilencer 4.1-GADPH vector using Lipofectamine (Invitrogen). After 48 h, the cells were trypsinized and split 1:10 into 60-mm dishes and cultured in the above media containing Geneticin (G418, 500 μg/ml). After 14 days, geneticin resistant colonies were isolated and expanded for histological examination.

Quantitative RT–PCR

Total RNA was isolated from cultured cells or mouse tissues using the Trizol Reagent (Invitrogene) according to the manufacturer's protocol and reverse transcripted to cDNA by using random primers and SuperScript III reverse transcriptase (Invitrogen). Quantification of human *Neu1* and *Neu4* mRNA in cultured cells and mouse tissues was performed using a LightCycler system (Roche, Germany) and the following two sets of primers: 5′-AGG TGG CCT CTA CCA TGT TG-3′ and 5′-GCA GCG GCA ATG GTA GTT AT-3′ (*Neu1*); 5′-TGC AGT ACT GGA GGA GCA CA-3′ and 5′-AGG TGT AAG CAG GAA CAA GCA-3′ (*Neu4*). β-Actin mRNA was used as a reference control.

In situ hybridization

Newborn brains were fixed in the Carnoy's fluid, embedded in paraffin and sectioned at 6 μM. Seven-week-old mice were anaesthetized and perfused via cardiac puncture with saline and then 4% paraformaldehyde. Whole brains were rapidly removed, post-fixed overnight and then processed to generate four sets of 20 μM adjacent coronal sections with a cryostat. *In situ* hybridization was performed using radioactive probes as previously described (47) on one out of two sections of newborn brain sets and selected adjacent sections from adult brains at an interval of 150 μM. The *Neu1* probe contained the entire 1.2 kb of mouse cDNA. The *Neu3* and *Neu4* probes corresponding to a 1.1-kb sequence fragments were generated by RT–PCR, using mouse newborn total brain RNA extracts and the following sets of primers: 5′-CTG ATG GAG GCC ACA TTA CC-3′ and 5′- TCC CCA CAC TCA AAC AAA CA-3′ (*Neu3*); 5′-AAG CTT GAC TGG GCC ACC TTT GCT-3′ and 5′-CTG CAG GCC AGC AAT GCC CCT GA-3′ (*Neu4*). The RNA probes were transcribed from linearized plasmids using either T7 or T3 RNA polymerase in the presence of [^{35}S]-UTP. Both sense and antisense transcripts were used for *Neu4* and only antisense transcripts for Neu1 and Neu3. After hybridization, slides were dipped in the emulsion and exposed for a period of 2 weeks.

Fractionation of brain tissues

Brains from 6-month-old wild-type and *Neu4*$^{-/-}$ mice were rapidly dissected, frozen in liquid nitrogen, homogenized in 1 ml of lysis buffer (5 mM MOPS pH 7.4, 250 mM sucrose, 1 mM EDTA, 0.1% Ethanol) and separated by centrifugation to the nuclear fraction and post-nuclear supernatant as described (48). Heavy organellar, light organellar and microsomal fractions were obtained by consequent centrifugation of post-nuclear supernatant at 5500*g* for 10 min, 18 000*g* for 30 min and 105 000*g* for 1 h.

Enzyme assays

Sialidase, β-glucosidase and β-hexosaminidase activities in cellular homogenates and in subcellular fractions from brain tissues of *Neu4*$^{-/-}$ and wild-type littermates mice were assayed using the corresponding fluorogenic 4-methylumbelliferyl glycoside substrates as previously described (23). Glutamate dehydrogenase (mitochondrial marker enzyme) activity in subcellular fractions from brain tissue was measured as described elsewhere (49). Sialidase activity against G_{M1}, G_{M2}, and G_{D1a} gangliosides and against total porcine brain gangliosides (all Avanti Polar

Lipids) was measured as described (17). The concentration of released sialic acid was measured by the thiobarbituric method (50). Protein concentration was determined according to Bradford (51).

Isolation and culturing of splenocytes

Fresh splenocytes were obtained by teasing the mouse spleens under aseptic conditions. Erythrocytes were removed by centrifugation over Ficoll-Paque Plus gradient and the remaining unfractionated nucleated spleen cells were washed twice with PBS and adjusted to a density of 7.5×10^5 of cells per milliliter of RPMI medium 1640 containing 10% of heat-inactivated FCS. To obtain splenocyte-derived macrophages, purified splenocytes were maintained at 2×10^6 of cells per well in six well tissue culture plates (Costar, Corning Inc., Corning, NY) at 37°C in a humidified atmosphere containing 5% CO2. After 7 days, non-adherent cells were removed by two washes with PBS and the adherent, differentiated macrophages were harvested in PBS by gentle scraping with a polyethylene cell scraper (Nalgene). The harvested cells were confirmed to have characteristic macrophage cell surface phenotypic markers (CD14+, CD206+) by flow cytometry. The macrophages from the knockout and wild-type mice were loaded for 72 h with total porcine brain gangliosides (Avanti Polar Lipids). The gangliosides were directly added to the culture medium at a final concentration of 0.2 mg/ml.

Transient expression of Neu4 in Tay-Sachs neuroglia cells

The immortalized human neuroglia cells obtained from normal healthy controls and a Tay-Sachs patient (26) grown in 100 mM Petri dishes were transfected with pCMV-SPORT6-Neu4 vector (50) or pCMV-SPORT6 vector as a mock control using Lipofectamine reagent according to the manufacturer's guidelines (Invitrogen). Forty-eight hours after transfection, the cells were incubated for 72 h with 3.3 nmol/ml fluorescently labeled $G_{M1,}$ prepared by Marchesini *et al*. (27), 10 μCi/ml of [^{3}H]labeled G_{M2} (American Radiolabeled Chemicals) or 0.2 mg/ml of total gangliosides from porcine brain (Avanti Polar Lipids). Alternatively the cells were metabolically labeled for 48 h with 3 μCi/ml of [^{14}C]serine (Amersham Bioscience).

Light and electron microscopy of cultured cells

Cultured cells were trypsinized, pelleted at 500*g* and fixed for 3 min in 2.5% glutaraldehyde. The cells were further pelleted by centrifugation for 5 min at 2300*g*. The supernatant was decanted and 5% glutaraldehyde added. Subsequent to 15 min incubation at 4°C, the cells were collected by centrifugation for 15 min at 21 000*g*. The resulting pellet was then incubated in 5% glutaraldehyde overnight at 4°C. The cells were post-fixed with osmium-ferrocyanide. Increasing concentrations of ethanol were used for subsequent dehydration. The cells were then embedded in Epon. Semi-thin sections (1 μm thick) were cut, mounted on slides, stained with toluidine blue, and visualized with a Leica DMS light microscope. Subsequently, ultrathin sections were cut and mounted on 200 mesh copper grids. Staining of the grids was done with uranyl acetate for 5 min, followed by lead citrate for 2 min. The grids were viewed on a Tecnai FEI electron microscope.

Electron microscopy of mouse tissues

Neu4 knockout mice and their wild-type littermates of 1, 4 and 6 months of age were anesthetized with sodium pentobarbital and sacrificed by exsanguinations. Lung, spleen, brain and liver were removed and fixed by immersion in 2.5% glutaraldehyde in 0.1 M cacodylate buffer for 48 h at 4°C. The tissues were embedded in Epon, cut and viewed on a Tecnai FEI electron microscope as described for the cultured cells.

Measurement of gangliosides in cell lysates and mouse tissues

Lipids were extracted by adding 1 ml of a chloroform/methanol mixture (1:1, v/v) to cell pellets or tissue lysates (mouse tissues were homogenized using a FastPrep-24 MP homogenizer). After thorough mixing, phase separation was induced by adding 0.65 ml of phosphate-buffered saline (PBS). After centrifugation at 500*g* for 15 min, the upper phase containing gangliosides was isolated. The lower phase was washed first with PBS and then with water. The upper phases were combined and passed through a Supelclean LC-18 column (Supelco). Gangliosides were eluted first using methanol and then the chloroform/methanol mixture. After evaporation under a stream of nitrogen, the residue was resuspended in 0.1 ml of the chloroform/methanol mixture and applied to a silica gel thin-layer chromatography (TLC) plate that was developed using chloroform/methanol/0.22% $CaCl_2$ (55:45:10, by vol.). After staining with orcinol or resorcinol, gangliosides were identified by comparing their Rf to those of authentic porcine brain ganglioside standards (Avanti Polar Lipids). Lipids present in the lower phase were separated by TLC using chloroform/methanol/ammonia/water (70:30:2:3, by vol.). When appropriate, radioactive lipids were first detected using a Berthold Tracemaster 20 radiochromatoscanner, then scraped from the plate and counted by liquid scintillation.

Statistical analysis

Statistical analysis has been performed using two-tailed *t*-test and ANOVA test.

SUPPLEMENTARY MATERIAL

Supplementary Material is available at HMG Online.

ACKNOWLEDGEMENTS

We acknowledge the help of Eve-Marie Charbonneau and Nicholas Cermakian in conducting the behavioral studies, and of Jacinthe Sirois and McGill Cancer Center Transgenic Mouse Core Facilities in producing the transgenic animals. We also thank Raffaela Ballarano for help in preparation of the manuscript and Mila Ashmarina for critical reading of

the manuscript and helpful advice. V.S. acknowledges a post-doctoral fellowship from the Fonds de la recherche en santé du Québec (FRSQ) and Fondation de l'Hôpital Sainte-Justine. A.V.P. is a National Investigator of FRSQ.

Conflict of Interest statement. None declared.

FUNDING

This work was supported in part by the operating grants from Canadian Institutes of Health Research (FRN 15079) to A.V.P. and from the Association Vaincre les Maladies Lysosomales to A.V.P and T.L., INSERM and Université Paul Sabatier to T.L. and from the Association Vaincre les Maladies Lysosomales, and the exchange program between Université de Montréal and Université Paul Sabatier to A.V.P., V.S. and T.L.

REFERENCES

1. Hakomori, S. (2003) Structure, organization, and function of glycosphingolipids in membrane. *Curr. Opin. Hematol.*, **10**, 16–24.
2. Kolter, T., Proia, R.L. and Sandhoff, K. (2002) Combinatorial ganglioside biosynthesis. *J. Biol. Chem.*, **277**, 25859–25862.
3. Schauer, R., Schmid, H., Pommerencke, J., Iwersen, M. and Kohla, G. (2001) Metabolism and role of O-acetylated sialic acids. *Adv. Exp. Med. Biol.*, **491**, 325–342.
4. Tettamanti, G. (2004) Ganglioside/glycosphingolipid turnover: new concepts. *Glycoconj. J.*, **20**, 301–317.
5. Pshezhetsky, A.V. and Ashmarina, M. (2001) Lysosomal multienzyme complex: biochemistry, genetics, and molecular pathophysiology. *Prog. Nucleic Acid Res. Mol. Biol.*, **69**, 81–114.
6. d'Azzo, A., Andria, G., Strisciuglio, G. and Galjaard, H. (2001) Galactosialidosis. In Scriver, C.R., Beaudet, A.L., Sly, W.S. and Valle, D. (eds), *Metabolic and Molecular Bases of Inherited Disease*. McGraw-Hill, New York, NY, pp. 3811–3826.
7. Thomas, G.H. (2001) Disorders of glycoprotein degradation: α-mannosidosis, β-mannosidosis, fucosidosis, and sialidosis. In Scriver, C.R., Beaudet, A.L., Sly, W.S. and Valle, D. (eds), *The Metabolic and Molecular Bases of Inherited Disease*. McGraw-Hill, New York, NY, pp. 3507–3534.
8. Miyagi, T. and Tsuiki, S. (1985) Purification and characterization of cytosolic sialidase from rat liver. *J. Biol. Chem.*, **260**, 710–6716.
9. Monti, E., Preti, A., Rossi, E., Ballabio, A. and Borsani, G. (1991) Cloning and characterization of NEU2, a human gene homologous to rodent soluble sialidases. *Genomics*, **57**, 137–143.
10. Tringali, C., Papini, N., Fusi, P., Croci, G., Borsani, G., Preti, A., Tortora, P., Tettamanti, G., Venerando, B. and Monti, E. (2004) Properties of recombinant human cytosolic sialidase HsNEU2. The enzyme hydrolyzes monomerically dispersed GM1 ganglioside molecules. *J. Biol. Chem.*, **279**, 3169–3179.
11. Akita, H., Miyagi, T., Hata, K. and Kagayama, M. (1997) Immunohistochemical evidence for the existence of rat cytosolic sialidase in rat skeletal muscles. *Histochem. Cell. Biol.*, **107**, 495–503.
12. Fanzani, A., Giuliani, R., Colombo, F., Zizioli, D., Presta, M., Preti, A. and Marchesini, S. (2003) Overexpression of cytosolic sialidase Neu2 induces myoblast differentiation in C2C12 cells. *FEBS Lett.*, **547**, 183–188.
13. Sato, K. and Miyagi, T. (1996) Involvement of an endogenous sialidase in skeletal muscle cell differentiation. *Biochem. Biophys. Res. Commun.*, **221**, 826–830.
14. Monti, E., Bassi, M.T., Papini, N., Riboni, M., Manzoni, M., Venerando, B., Croci, G., Preti, A., Ballabio, A., Tettamanti, G. and Borsani, G. (2000) Identification and expression of NEU3, a novel human sialidase associated to the plasma membrane. *Biochem. J.*, **349**, 343–351.
15. Wada, T., Yoshikawa, Y., Tokuyama, S., Kuwabara, M., Akita, H. and Miyagi, T. (1999) Cloning, expression, and chromosomal mapping of a human ganglioside sialidase. *Biochem. Biophys. Res. Commun.*, **261**, 21–27.
16. Wang, Y., Yamaguchi, K., Wada, T., Hata, K., Zhao, X., Fujimoto, T. and Miyagi, T. (2002) A close association of the ganglioside-specific sialidase Neu3 with caveolin in membrane microdomains. *J. Biol. Chem.*, **277**, 26252–26259.
17. Schneider-Jakob, H.R. and Cantz, M. (1991) Lysosomal and plasma membrane ganglioside GM3 sialidases of cultured human fibroblasts. Differentiation by detergents and inhibitors. *Biol. Chem. Hoppe-Seyler*, **372**, 443–450.
18. Kopitz, J., von Reitzenstein, C., Sinz, K. and Cantz, M. (1996) Selective ganglioside desialylation in the plasma membrane of human neuroblastoma cells. *Glycobiology*, **6**, 367–376.
19. Kopitz, J., von Reitzenstein, C., Burchert, M., Cantz, M. and Gabiu, H.J. (1998) Galectin-1 is a major receptor for ganglioside GM1, a product of the growth-controlling activity of a cell surface ganglioside sialidase, on human neuroblastoma cells in culture. *J. Biol. Chem.*, **273**, 11205–11211.
20. Wu, G. and Ledeen, R.W. (1991) Stimulation of neurite outgrowth in neuroblastoma cells by neuraminidase: putative role of GM1 ganglioside in differentiation. *J. Neurochem.*, **56**, 95–104.
21. Kakugawa, Y., Wada, T., Yamaguchi, K., Yamanami, H., Ouchi, K., Sato, I. and Miyagi, T. (2002) Up-regulation of plasma membrane-associated ganglioside sialidase (Neu3) in human colon cancer and its involvement in apoptosis suppression. *Proc. Natl Acad. Sci. USA*, **99**, 10718–10723.
22. Sasaki, A., Hata, K., Suzuki, S., Sawada, M., Wada, T., Yamaguchi, K., Obinata, M., Tateno, H., Suzuki, H. and Miyagi, T. (2003) Overexpression of plasma membrane-associated sialidase attenuates insulin signaling in transgenic mice. *J. Biol. Chem.*, **278**, 27896–27902.
23. Seyrantepe, V., Landry, K., Trudel, S., Hassan, J.A., Morales, C.R. and Pshezhetsky, A.V. (2004) Neu4, a novel human lysosomal lumen sialidase, confers normal phenotype to sialidosis and galactosialidosis cells. *J. Biol. Chem.*, **279**, 37021–37029.
24. Yamaguchi, K., Hata, K., Koseki, K., Shiozaki, K., Akita, H., Wada, T., Moriya, S. and Miyagi, T. (2005) Evidence for mitochondrial localization of a novel human sialidase (NEU4). *Biochem. J*, **390**, 85–93.
25. Kolter, T. and Sandhoff, K. (2005) Principles of lysosomal membrane digestion: stimulation of sphingolipid degradation by sphingolipid activator proteins and anionic lysosomal lipids. *Ann. Rev. Cell. Dev. Biol.*, **21**, 81–103.
26. Hoffman, L., Amsterdam, M.D. and Schneck, L. (1976) G_{M2} ganglioside in fetal Tay-Sachs disease brain cultures: a model system for the disease. *Brain. Res.*, **111**, 109–117.
27. Marchesini, S., Demasi, L., Cestone, P., Preti, A., Agmon, V., Dagan, A., Navon, R. and Gatt, S. (1994) Sulforhodamine GM1-ganglioside: synthesis and physicochemical properties. *Chem. Phys. Lipids*, **72**, 143–152.
28. Comelli, E.M., Amado, M., Lustig, S.R. and Paulson, J.C. (2003) Identification and expression of Neu4, a novel murine sialidase. *Gene*, **321**, 155–161.
29. Miklyaeva, E.I., Dong, W., Bureau, A., Fattahie, R., Xu, Y., Su, M., Fick, G.H., Huang, J.Q., Igdoura, S., Hanai, N. and Gravel, R.A. (2004) Late onset Tay-Sachs disease in mice with targeted disruption of the Hexa gene: behavioral changes and pathology of the central nervous system. *Brain Res.*, **1001**, 37–50.
30. Monti, E., Bassi, M.T., Bresciani, R., Civini, S., Croci, G.L., Papini, N., Riboni, M., Zanchetti, G., Ballabio, A., Preti, A. *et al.* (2004) Molecular cloning and characterization of NEU4, the fourth member of the human sialidase gene family. *Genomics*, **83**, 445–453.
31. Igdoura, S.A., Mertineit, C., Trasler, J.M. and Gravel, R.A. (1999) Sialidase-mediated depletion of GM2 ganglioside in Tay-Sachs neuroglia cells. *Hum. Mol. Genet.*, **8**, 1111–1116.
32. Fingerhut, R., van der Horst, G.T., Verheijen, F.W. and Conzelmann, E. (1992) Degradation of gangliosides by the lysosomal sialidase requires an activator protein. *Eur. J. Biochem.*, **208**, 623–629.
33. Hiraiwa, M., Uda, Y., Nishizawa, M. and Miyatake, T. (1987) Human placental sialidase: partial purification and characterization. *J. Biochem. (Tokyo)*, **101**, 1273–1279.
34. Hiraiwa, M., Nishizawa, M., Uda, Y., Nakajima, T. and Miyatake, T. (1988) Human placental sialidase: further purification and characterization. *J. Biochem. (Tokyo)*, **103**, 86–90.
35. de Geest, N., Bonten, E., Mann, L., de Sousa-Hitzler, J., Hahn, C. and d'Azzo, A. (2002) Systemic and neurologic abnormalities distinguish the lysosomal disorders sialidosis and galactosialidosis in mice. *Hum. Mol. Genet.*, **11**, 1455–1464.

36. Zhou, X.Y., Morreau, H., Rottier, R., Davis, D., Bonten, E., Gillemans, N., Wenger, D., Grosveld, F.G., Doherty Suzuki, K. *et al.* (1995) Mouse model for the lysosomal disorder galactosialidosis and correction of the phenotype with overexpressing erythroid precursor cells. *Genes Dev.*, **9**, 2623–2634.
37. Butler, J.D., Vanier, M.T. and Pentchev, P.G. (1993) Niemann-Pick C disease: cystine and lipids accumulate in the murine model of this lysosomal cholesterol lipidosis. *Biochem. Biophys. Res. Commun.*, **196**, 154–159.
38. Harzer, K., Massenkeil, G. and Frohlich, E. (2003) Concurrent increase of cholesterol, sphingomyelin and glucosylceramide in the spleen from non-neurologic Niemann-Pick type C patients but also patients possibly affected with other lipid trafficking disorders. *FEBS Lett.*, **537**, 177–181.
39. Vanier, M.T. (1983) Biochemical studies in Niemann-Pick disease. I. Major sphingolipids of liver and spleen. *Biochim. Biophys. Acta*, **750**, 178–184.
40. Devendra, G. and Spragg, R.G. (2002) Lung surfactant in subacute pulmonary disease. *Respir. Res.*, **3**, 19.
41. Weaver, T.E., Na, C.L. and Stahlman, M. (2002) Biogenesis of lamellar bodies, lysosome-related organelles involved in storage and secretion of pulmonary surfactant. *Semin. Cell Dev. Biol.*, **13**, 263–270.
42. Streit, W.J. (2001) Microglia and macrophages in the developing CNS. *Neurotoxicology*, **22**, 619–624.
43. Shiozaki, K., Koseki, K., Yamaguchi, K.Y., Shiozaki, M. and Miyagi, T. (2006) Developmental change of neu4 expression in mouse brain and its involvement in neuronal cell development (Abstract). *Trends Glycosci. Glycotechnol.*, **18**, S43.
44. Phaneuf, D., Wakamatsu, N., Huang, J.Q., Borowski, A., Peterson, A.C., Fortunato, S.R., Ritter, G., Igdoura, S.A., Morales, C.R., Benoit, G. *et al.* (1996) Dramatically different phenotypes in mouse models of human Tay-Sachs and Sandhoff diseases. *Hum. Mol. Genet.*, **5**, 1–14.
45. Sango, K., Yamanaka, S., Hoffmann, A., Okuda, Y., Grinberg, A., Westphal, H., McDonald, M.P., Crawley, J.N., Sandhoff, K., Suzuki, K. and Proia, R.L. (1995) Mouse models of Tay-Sachs and Sandhoff diseases differ in neurologic phenotype and ganglioside metabolism. *Nat. Genet.*, **11**, 170–176.
46. Zhao, Q. and Morales, C.R. (2000) Identification of a novel sequence involved in lysosomal sorting of the sphingolipid activator protein prosaposin. *J. Biol. Chem.*, **275**, 24829–24839.
47. Fan, C.M., Kuwana, E., Bulfone, A., Fletcher, C.F., Copeland, N.G., Jenkins, N.A., Crews, S., Martinez, S., Puelles, L., Rubenstein, J.L. and Tessier-Lavigne, M. (1996) Expression patterns of two murine homologs of Drosophila single-minded suggest possible roles in embryonic patterning and in the pathogenesis of Down syndrome. *Mol. Cell. Neurosci.*, **7**, 1–16.
48. Kovacs, W.J., Faust, P.L., Keller, G.A. and Krisans, S.K. (2001) Purification of brain peroxisomes and localization of 3-hydroxy-3-methylglutaryl coenzyme A reductase. *Eur. J. Biochem.*, **268**, 4850–4859.
49. Schmidt, E. (1974) Glutamate dehydrogenase. In Bergmeyer, H.V. (ed.), *Methods of Enzymatic Analysis*. Verlag Chemie, Weinheim, Germany, pp. 650–656.
50. Manzi, A.E. (2003) Preparation and Analysis of Glycoconjugates. In Ausubel, F.M., Brent, R., Kingston, R.E., Moore, D.D., Seidman, J.G., Smith, J.A. and Struhl, K. (eds), *Current Protocols in Molecular Biology*. John Wiley & Sons, Inc., New York, NY, Vol. 3, pp. 17.18.8–17.18.10.
51. Bradford, M.M. (1976) A rapid and sensitive method for the quantitation of microgram quantities of protein utilizing the principle of protein-dye binding. *Anal. Biochem.*, **72**, 248–254.